Purdue University

Purdue e-Pubs

International Refrigeration and Air Conditioning Conference

School of Mechanical Engineering

2022

Condensation Heat Transfer Coefficient Measurements and Flow Pattern Visualizations of R515B and R450A Inside a 3.4 mm Diameter Channel

Marco Azzolin

Arianna Berto

Stefano Bortolin

Nicolò Mattiuzzo

Davide Del Col

Follow this and additional works at: https://docs.lib.purdue.edu/iracc

Azzolin, Marco; Berto, Arianna; Bortolin, Stefano; Mattiuzzo, Nicolò; and Del Col, Davide, "Condensation Heat Transfer Coefficient Measurements and Flow Pattern Visualizations of R515B and R450A Inside a 3.4 mm Diameter Channel" (2022). *International Refrigeration and Air Conditioning Conference.* Paper 2426.
https://docs.lib.purdue.edu/iracc/2426

This document has been made available through Purdue e-Pubs, a service of the Purdue University Libraries. Please contact epubs@purdue.edu for additional information.
Complete proceedings may be acquired in print and on CD-ROM directly from the Ray W. Herrick Laboratories at https://engineering.purdue.edu/Herrick/Events/orderlit.html

CONDENSATION HEAT TRANSFER COEFFICIENT MEASUREMENTS AND FLOW PATTERN VISUALIZATIONS OF R515B AND R450A INSIDE A 3.4 mm DIAMETER CHANNEL

Marco AZZOLIN*, Arianna BERTO, Stefano BORTOLIN, Nicolò MATTIUZZO, Davide DEL COL

University of Padova, Department of Industrial Engineering
Via Venezia 1, 35131 - Padova, Italy

* Corresponding Author: marco.azzolin@unipd.it

ABSTRACT

An alternative low Global Warming Potential (GWP) refrigerant that could be used to replace R134a in heat pumps, refrigeration and air-conditioning systems is the hydrofluoroolefin R1234ze(E). As a drawback, R1234ze(E) is classified as a mildly flammable fluid (A2L ANSI/ASHRAE classification) and it presents a lower volumetric cooling capacity compared to R134a. In the search for non-flammable R134a substitutes, hydrofluorocarbon/hydrofluoroolefin binary mixtures can be considered. R515B (R1234ze(E)/R227ea at 91.1/8.9% by mass) and R450A (R1234ze(E)/R134a at 58.0/42.0% by mass) are two alternatives classified as A1 (not flammable). R515B is an azeotropic mixture with $GWP_{100\text{-}years}$ = 299, whereas R450A is a near-azeotropic blend (temperature glide 0.6 K at 40 °C) with $GWP_{100\text{-}years}$ = 547.
In this work, condensation tests are performed with R515B and R450A inside a circular cross-section channel with an inner diameter equal to 3.4 mm. The test section is composed of two copper heat exchangers designed for the measurement of the quasi-local heat transfer coefficient. A glass tube, located between the two diabatic parts of the test section allows the visualization of the two-phase flow patterns by a high-speed camera. Heat transfer coefficients are measured at 40 °C mean saturation temperature and mass flux between 50 and 300 kg m^{-2} s^{-1}. The prediction accuracy of condensation heat transfer models is then assessed against the experimental results. Measured heat transfer coefficients are also compared with those of R1234ze(E) at the same operative conditions.
Regarding the diameter of the present test tube, it is worthy to point out that small diameter tubes are often employed in finned coil heat exchangers and minichannel heat exchangers are a common solution for air-cooled condensers.

1. INTRODUCTION

Considering the increased concern about the greenhouse effect, in the last years, many efforts have been put to find alternatives for the high global warming potential (GWP) hydrofluorocarbons (HFCs). Hydrofluoroolefins (HFOs), R1234ze(E) and R1234yf emerged as possible substitutes for R134a. Several studies have been conducted to compare the heat transfer performance of these fluids with R134a, finding that they have similar behaviour (Del Col et al., (2015), Diani et al., (2018a), Diani et al., (2018b)).
However, R1234ze(E) and R1234yf are classified by ANSI/ASHRAE standard 34 as A2L mildly flammable fluids. The possibility to create A1 non-flammable blends of low GWP refrigerants is sought by the industries since they can be used as drop-in fluids in existing systems. Among the A1 low-GWP mixtures, R450A (R1234ze(E)/R134a at 58.0/42.0% by mass) and R515B (R1234ze(E)/R227ea at 91.1/8.9% by mass) can be counted as a possible replacement of R134a in vapour compression cycles (Mateu-Royo et al. (2021) and Makhnatch et al. (2019)). However, few studies (Jacob et al., 2019) investigate the heat transfer during condensation of these mixtures and no works present flow pattern visualizations.
In the present work, the heat transfer coefficients during condensation and the flow pattern visualizations of R450A and R515B have been evaluated in a 3.38 mm diameter horizontal channel. Measured heat transfer coefficients are also compared with those of R1234ze(E) at the same operative conditions. The experimental points are also used to assess the prediction accuracy of analytical models that can be found in the literature.

2. EXPERIMENTAL SETUP AND DATA REDUCTION

The experimental tests have been conducted in a test section that has an internal diameter equal to 3.38 mm and that consists of two heat exchangers separated by a glass window that allows to visualize the flow pattern. The first heat exchanger is subdivided into three sectors while the second heat exchanger is subdivided into two sectors. In the test section, the water flows in an external annulus whereas the refrigerant flows in counter-current inside the copper tube. In each sector, on the water side, a thermopile and two T-type thermocouples (to double-check the water temperature difference $\Delta T_{w,i}$) are installed and they allow to perform an energy balance on the water side (the water flow rate is measured with a Coriolis effect mass flow meter). In each sector, six thermocouples have been installed to measure the wall temperatures, while the refrigerant temperature is deduced by the saturation pressure measured by the pressure transducers. Thus, the quasi-local refrigerant heat transfer coefficient for each sector is obtained as reported in Eq. 1:

$$\alpha_i = \frac{m_w \cdot c \cdot \Delta T_{w,i}}{\left(T_{sat} - T_{wall}\right) \cdot \pi \cdot d \cdot L} \tag{1}$$

where the numerator is the heat flow rate exchanged ($q_{w,i}$) in the sector calculated considering the energy balance on the water side. To calculate the vapor quality at the outlet of the i-th sector the following equation is used:

$$h_{i,out} = h_{i,in} - \frac{q_{w,i}}{\dot{m}_r} \tag{2}$$

In equation (2), the enthalpy at the outlet of each sector is calculated from the heat exchanged in the sector, the refrigerant mass flow rate $\dot{m}_r$ and the inlet enthalpy $h_{i,in}$, which is assumed equal to the one at the outlet of the previous sector. The refrigerant enters the first sector as superheated vapor and its enthalpy is determined from pressure and temperature measurements. More details regarding the experimental setup and the data reduction procedure are available in Azzolin et al. (2019) and in Azzolin et al. (2022).

Following the JCGM (2008) guide, the uncertainty analysis of the measured and calculated parameters has been evaluated. All the reported expanded uncertainty has been calculated considering a coverage factor k=2, thus assuming a confidence level of 95%. Regarding the heat transfer coefficient, the average expanded uncertainty of the present database is around ±2% and the maximum uncertainty value is equal to ±5.5%; regarding the vapor quality, the average expanded uncertainty amounts to ±0.01 with a maximum value equal to ±0.025.

The fluids tested in the present work are two blends with R1234ze(E) as major components. This refrigerant is an HFO, it presents a $GWP_{100\text{-years}}$ lower than 1 and it is classified as mildly-flammable A2L by the ANSI/ASHRAE classification. To overcome this problem, mixtures of R1234ze(E) have been considered and the two blends studied in this work are non-flammable (A1 class). The first blend is R450A which is composed of R1234ze(E) and R134a at 58.0/42.0% by mass. R450A is a near-azeotropic blend: the temperature glide at 8.95 bar is equal to 0.63 K. The second blend investigated in the present work is R515B which is composed of R1234ze(E) and R227ea (91.1/8.9% by mass) and it is an azeotropic mixture. The thermodynamic and transport properties of the tested mixtures and of the pure components are reported in Table 1 at a mean saturation temperature equal to 40 °C. The two selected blends R515B and R450A present a significantly lower value of $GWP_{100\text{-years}}$ if compared to the one of R134a ($GWP_{100\text{-years}}$ =1300): R515B and R450A have a global warming potential considering a time period of 100 years respectively equal to 299 and 547.

When considering an ideal vapor compression cycle, operating between 40 °C condensation temperature and 0 °C evaporation temperature, with 5 K subcooling and 10 K superheating, it is possible to calculate that the volumetric cooling capacity of the fluid R450A is slightly higher (+18%) with respect to R1234ze(E) and R515B.

To study the heat transfer coefficients during condensation, experimental tests have been conducted at a mean saturation temperature equal to 40 °C for both the mixtures (this condition corresponds to 7.62 bar saturation pressure for R515B and to 8.95 bar saturation pressure for R450A). The experimental tests have been performed at mass flux equal to 50, 100, 200 and 300 kg m^{-2} s^{-1} varying the coolant water temperature and the water mass flow rate in the test section.

Table 1: Properties of pure base fluids and two tested mixtures calculated at 40 °C mean saturation temperature by NIST Refprop (2010).

Fluid	p_{sat} [bar]	ρ_L [kg m^{-3}]	ρ_V [kg m^{-3}]	λ_L [mW m^{-1} K^{-1}]	μ_L [µPa s]	T_{dew} [°C]	Glide [K]
R1234ze(E)	7.66	1111.5	40.64	69.21	157.89	40	-
R134a	10.17	1146.7	50.09	74.72	161.45	40	-
R515B	7.62	1128.3	41.66	68.301	159.88	40	-
R450A	8.95	1122.7	46.12	71.08	157.34	40.35	0.63

3. FLOW PATTERNS VISUALIZATIONS

The borosilicate glass tube placed between the two heat exchangers allows to visualize the flow pattern when varying the mass flux and the vapor quality at the outlet of the first heat exchanger. Photron® FASTCAM Mini UX100 high-speed camera coupled with 100 mm Tokina® macro lens has been employed to investigate the flow patterns. To improve the brightness of the images captured by the high-speed camera, a LED light source has been used with a light diffusion system.

The obtained flow pattern visualizations for R515B and R450A are reported in Fig.1 and Fig.2 respectively. As it can be seen, the flow regime for the different blends can be classified as follows:

- At low mass velocities (G = 50 kg m^{-2} s^{-1}), when the vapour quality is below 0.2, the flow is intermittent: liquid plugs and elongated smooth bubbles can be detected. When the vapor quality increases, the flow regime becomes stratified-smooth, with the liquid film thicker at the bottom part of the tube.
- Considering the visualization at G = 100 kg m^{-2} s^{-1}, the flow is stratified-wavy and stratified-smooth. The liquid film at the bottom of the channel is still thicker and, when the vapor quality decreases, the waves at the interface reduce in amplitude.
- At G = 200 kg m^{-2} s^{-1} and high vapor qualities, annular flow is observed. When decreasing the vapor quality the flow pattern is in transition between stratified-wavy and annular flow. The transition occurs at similar vapor qualities for the tested mixture, at x = 0.49 for R515B and at x = 0.52 for R450A.
- At the highest tested mass flux, G = 300 kg m^{-2} s^{-1}, the flow is identified as annular in all the range of vapor quality investigated.

The flow patterns recorded in the same test section for the pure R1234ze(E) can be found in Azzolin et al. (2022).

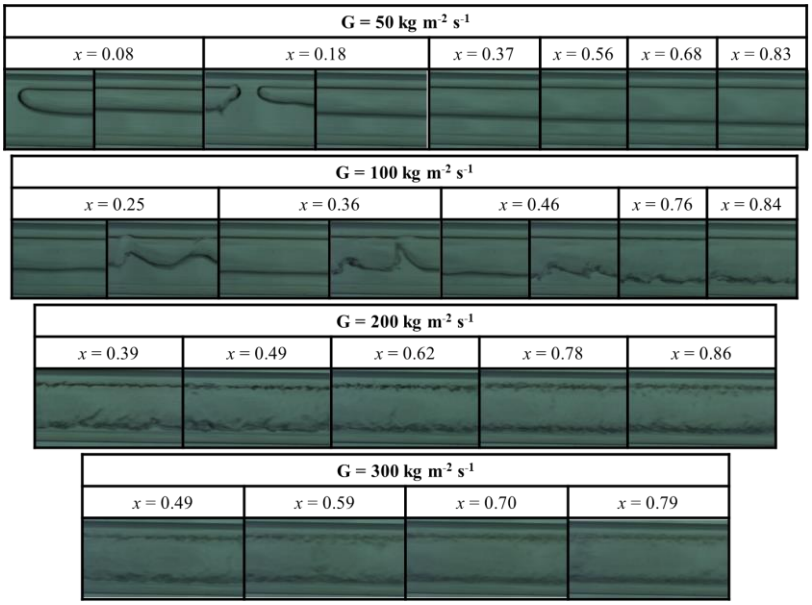

Figure 1: Flow pattern visualizations of R515B during condensation at 40 °C saturation temperature inside the 3.4 mm internal diameter channel when varying vapour quality and mass flux (50 kg m^{-2} s^{-1} < G < and 300 kg m^{-2} s^{-1}).

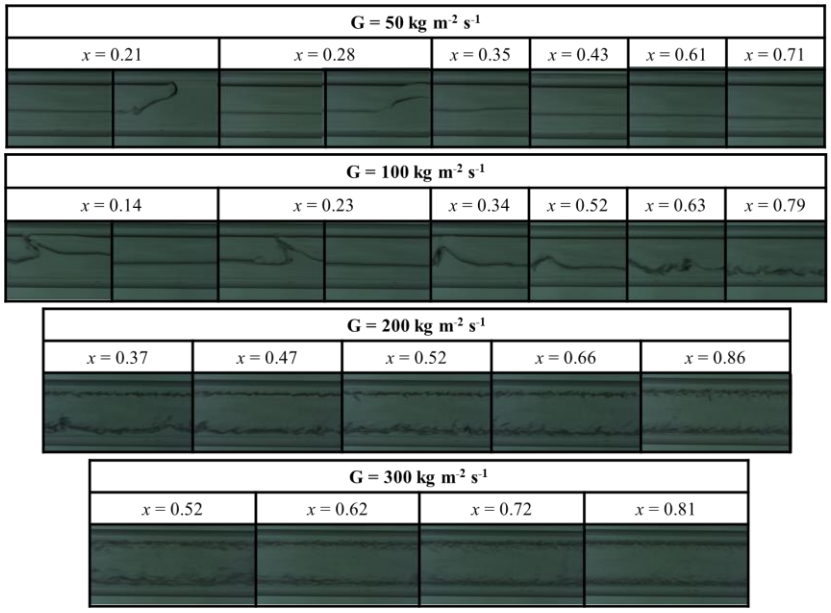

Figure 2: Flow pattern visualization of R450A during condensation at 40 °C saturation temperature inside the 3.4 mm internal diameter channel when varying vapour quality and mass flux (50 kg m^{-2} s^{-1} < G < and 300 kg m^{-2} s^{-1}).

4. CONDENSATION HEAT TRANSFER COEFFICIENTS RESULTS

The experimental condensation heat transfer coefficients of the two refrigerant blends evaluated in the 3.38 mm internal diameter channel are reported in Fig. 3a. Considering the experimental data for both the tested mixtures, the heat transfer coefficient increases when the mass flux becomes higher. Indeed, increasing the mass flux from 200 to 300 kg m^{-2} s^{-1}, the average increase of the heat transfer coefficient is around 40% for R515B and 35% for R450A. When the mass flux is increased from 50 kg m^{-2} s^{-1} to 100 kg m^{-2} s^{-1} the average enhancement of the heat transfer coefficient is reduced to 13% for both the blends. This can be explained by taking into account the flow pattern visualizations reported in Fig. 1 and Fig. 2. At mass flux equal to 200 kg m^{-2} s^{-1} and 300 kg m^{-2} s^{-1} the flow pattern is annular or in the transition between annular and stratified wavy. In this case, condensation is dominated by the vapor shear stress. When the mass flux is equal to 100 kg m^{-2} s^{-1} and 50 kg m^{-2} s^{-1} the flow pattern is stratified-wavy or stratified-smooth. In this case, the condensation process starts to be affected by the gravity force which acts to drain the liquid from the top of the channel down to the bottom: in these operative conditions, the mass flux has a lower influence on the heat transfer coefficient. However, when gravity starts to control the condensation process, the heat transfer coefficient depends on the difference between the saturation and the wall temperature. Figure 3b reports the heat transfer coefficients at G = 50 kg m^{-2} s^{-1} when varying the saturation-to-wall temperature difference. When considering R515B, the average heat transfer coefficient measured with saturation-to-wall temperature difference (ΔT) in the range 4 - 5.5 K is 11 % higher than the heat transfer coefficient obtained with ΔT between 7 and 9 K. When considering R450A, the average heat transfer coefficient with ΔT = 4 – 5.5 K is 15.7 % higher than the one measured with saturation-to-wall temperature difference in the interval 7 -10 K. It must be noted that experimental data reported in Figure 3a have been selected considering a ΔT higher than 6.5 K.

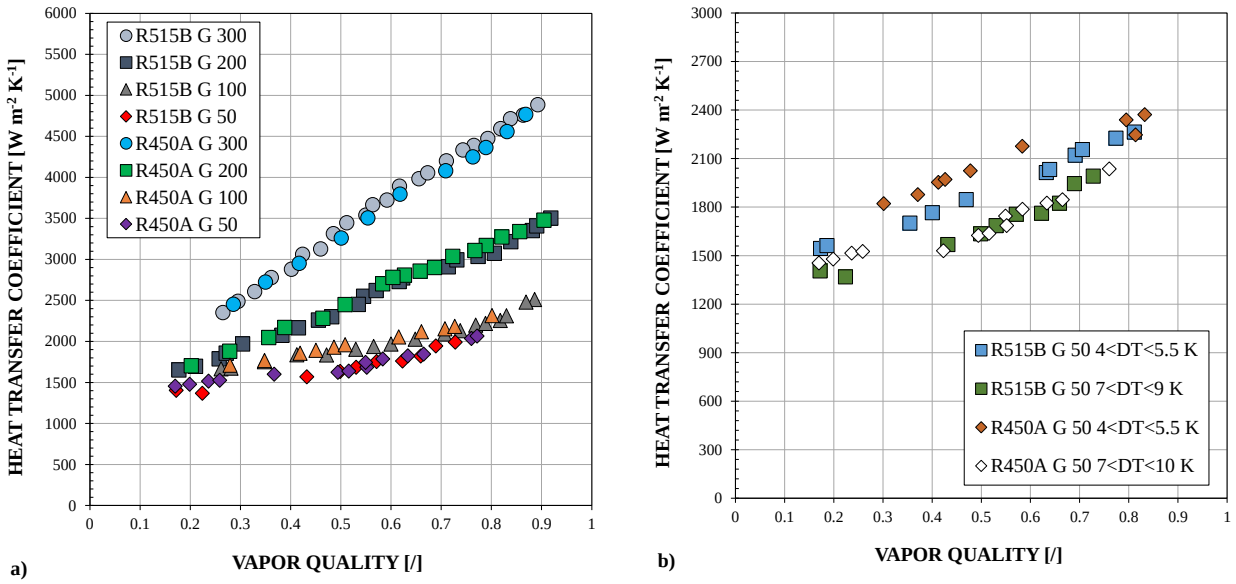

Figure 3: a) Condensation heat transfer coefficients of R515B and R450A during condensation at 40 °C saturation temperature in a 3.4 mm internal diameter horizontal channel for mass flux from 50 to 300 kg m^{-2} s^{-1}. b) Effect of the saturation-to-wall temperature difference (ΔT) on the condensation heat transfer coefficient at 50 kg m^{-2} s^{-1}. G is the mass flux [kg m^{-2} s^{-1}].

The heat transfer coefficients of R515B and R450A have been compared to those measured with R1234ze(E) in the same operative conditions. The heat transfer coefficients of R1234ze(E) used for this comparison are reported in Azzolin et al. (2022) and they have been measured at a saturation temperature equal to 40 °C in the same experimental setup. The comparison between the tested refrigerant mixtures with R1234ze(E) is reported in Figure 4. The mass fluxes selected are G = 50 kg m^{-2} s^{-1} and G = 300 kg m^{-2} s^{-1}, and the ratio of the heat transfer coefficients has been calculated for vapor quality ranging between 0.25 to 0.75. To perform this comparison, the measured heat transfer coefficients reported in Fig. 3 and those of R1234ze(E) have been interpolated to allow the calculation of the heat transfer coefficient at the same value of vapour quality.

As can be seen in Figure 4, there is not a remarkable difference between the measured HTCs of the two fluids. The mixture R515B presents slightly lower heat transfer coefficients with respect to R1234ze(E). Indeed, the heat transfer coefficient of R515B is, on average, 4.5 % lower than that of R1234ze(E) at 300 kg m^{-2} s^{-1} and 1.5 % lower at 50 kg m^{-2} s^{-1}. The reduced difference in the heat transfer coefficient can be explained by looking at the properties of the two fluids reported in Table 1: the liquid thermal conductivity and the vapor density present similar values.

Fig. 4b reports the same comparative analysis for R450A and R1234ze(E). With respect to R1234ze(E), at mass flux equal to 300 kg m^{-2} s^{-1}, the heat transfer coefficient of R450A is, on average, 6 % lower. At G = 300 kg m^{-2} s^{-1} the flow regime is annular and the condensation is controlled by the shear stress; thus the lower vapor density of R1234ze(E) leads to higher heat transfer coefficients compared to R450A. At G = 50 kg m^{-2} s^{-1} the heat transfer coefficient for R450A is higher than that of R1234ze(E) when the vapor quality is lower than 0.45; this is due to the higher liquid thermal conductivity of R450A compared to R1234ze(E). When the vapor quality is higher than 0.5, at G = 50 kg m^{-2} s^{-1}, the heat transfer coefficients are similar or slightly lower for the R450A: the lower vapour density of R1234ze(E) causes higher vapor velocities and this leads to higher heat transfer coefficient with respect to R450A.

However, the maximum heat transfer coefficient reduction for R515B and R450A compared to R1234ze(E) never exceeds 8%. It must be considered that this comparison is done at the same mass flux and vapor quality and thus pressure drop (during condensation the pressure drop affects the saturation temperature and thus the driving temperature difference of the heat transfer process) among the fluids should be accounted for.

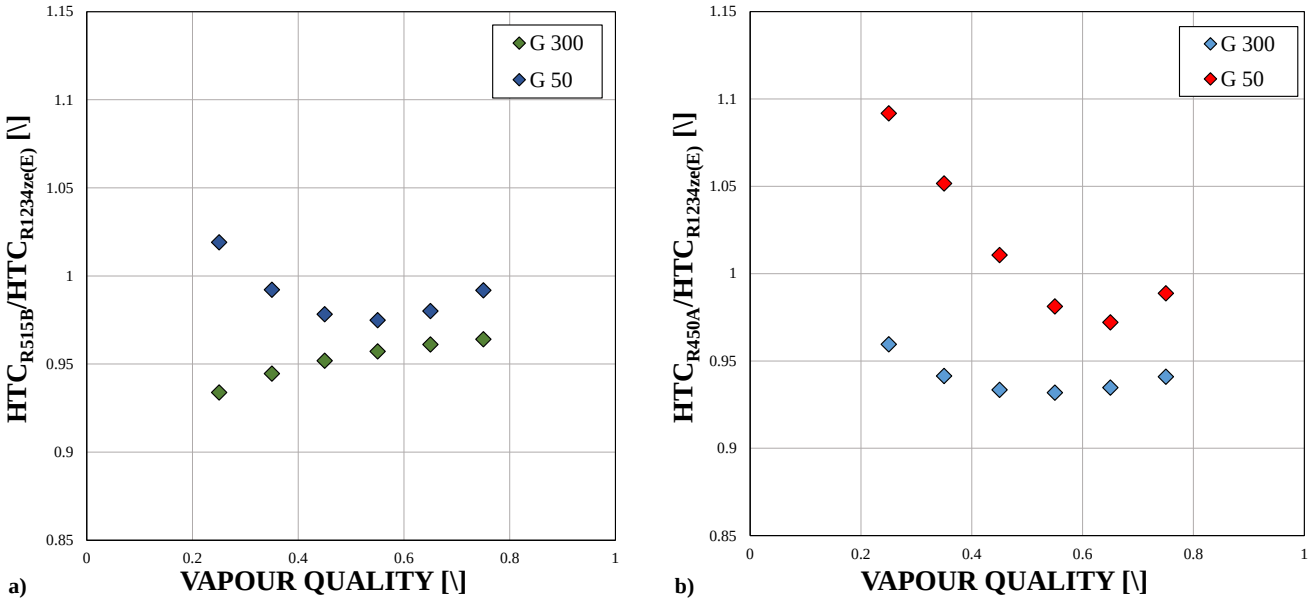

Figure 4: Ratio between the measured condensation heat transfer coefficients of the blends and those of R1234ze(E) in the 3.4 mm internal diameter channel, saturation temperature equal to 40 °C. a) ratio between heat transfer coefficient of R515B and R1234ze(E); b) ratio between heat transfer coefficient of R450A and R1234ze(E)

6. COMPARISON WITH CONDENSATION MODELS

The experimental data of the tested mixtures have been compared against the predictions of two models available in the literature: the Cavallini et al. (2006) model and the Thome et al. (2003) model. Both models are based on flow regimes maps. In the case of Cavallini et al. (2006) the calculation of the heat transfer coefficient is based on the identification of two different regimes: ΔT-independent region and the ΔT-dependent region. In the ΔT-independent region, the heat transfer coefficient is predicted as the liquid phase heat transfer coefficient corrected by a two-phase multiplier. In the ΔT-dependent region, the heat transfer coefficient is obtained considering the heat transfer coefficient of the ΔT-independent region and the fully stratified flow heat transfer coefficient. The transition between the two regions is a function of the Martinelli parameter.

The model reported in Thome et al. (2003) is based on the flow pattern map described in El Hajal et al. (2003). This model calculates the heat transfer coefficient as a combination of two terms: a convective heat transfer coefficient and a film condensation heat transfer coefficient. The contribution of these two terms depends on the flow regime inside the tube. The film condensation heat transfer coefficient is evaluated from the Nusselt (1916) theory. The combination of the stratified-flow and convective terms is done with geometrical assumptions on the value of the angle inside the tube at which the transition between falling film and convective boundaries occurs.

The results of the predictions from the Cavallini et al. (2006) model are displayed in Fig. 5. Since the two mixtures have a null or negligible temperature glide, the model has been applied without the introduction of correction factors to account for the additional mass transport resistance. The model shows a good agreement with the experimental data, predicting the condensation heat transfer coefficient with a mean absolute deviation equal to 4.8% for R515B and equal to 3.2% for R450A. The model gives very accurate predictions at mass fluxes equal to 200 kg m^{-2} s^{-1} and 300 kg m^{-2} s^{-1} with a mean absolute deviation lower than 3 % and a mean relative deviation equal to -2.9%. At the mass fluxes lower or equal to 100 kg m^{-2} s^{-1}, the mean deviation is equal to -6.6 % and -4.5 %, while the mean absolute deviation is 6.6 % and 5.1 % for R515B and R450A respectively. The maximum value of the average deviation has been found at G = 100 kg m^{-2} s^{-1} and it is equal to 17.32 % for R515A and equal to 17.6 % for R450A.

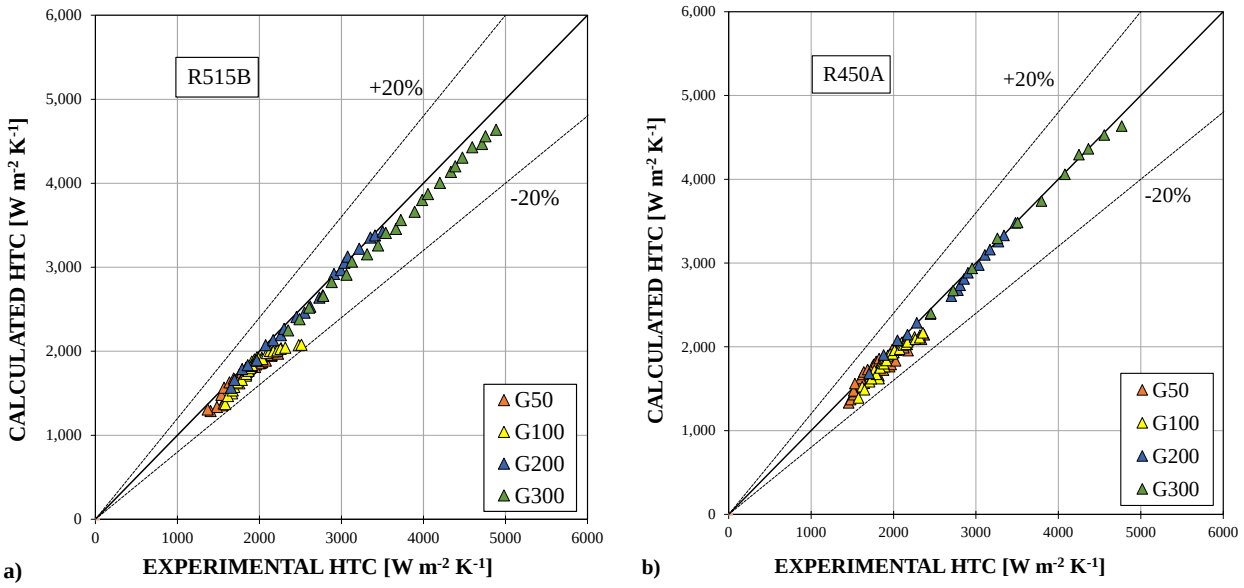

Figure 5: Comparison of the experimental heat transfer coefficients with the model by Cavallini et al. (2006) at 40 °C saturation temperature in the 3.4 mm diameter test section. a) Data for R515B; b) data for R450A.

In Fig. 6 the comparison between the condensation heat transfer coefficients calculated with Thome et al. (2003) model and the experimental data is reported. When considering this model, the average deviations are equal to 5.4% and 6% for R515B and R450A respectively. The mean absolute deviations are equal to 8.5% for both fluids. At G=50 kg m^{-2} s^{-1} the model displays higher deviations compared to the Cavallini et al. (2006) model: for R515B the average deviation is equal to 16% while for R450A it is even higher (18.8%). The maximum errors occur at 50 kg m^{-2} s^{-1} and are equal to 28.8% for R515B and 29.9% for R450A.

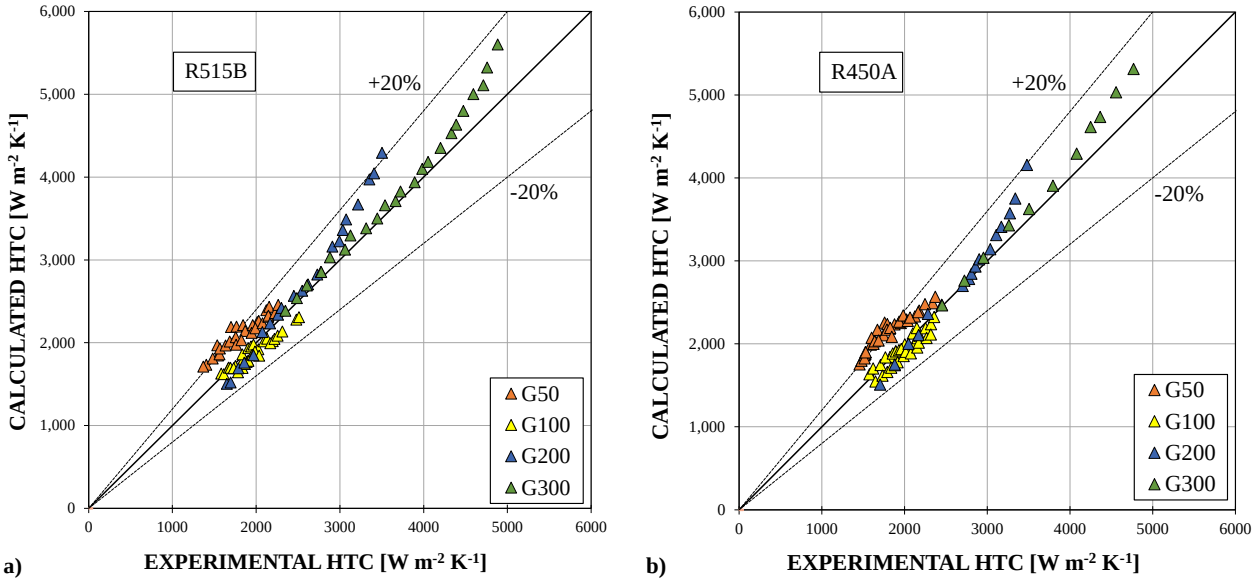

Figure 6: Comparison of the experimental heat transfer coefficient with the model by Thome et al. (2003) at saturation temperature equal to 40 °C in the 3.4 mm diameter test section. a) Data for R515B; b) data for R450A.

7. CONCLUSIONS

This paper presents an experimental study on condensation heat transfer of two blends R515B (R1234ze(E)/R227ea at 91.1/8.9% by mass) and R450A (R1234ze(E)/R134a at 58.0/42.0% by mass). The mixture R515B is azeotropic and its $GWP_{100\text{-years}}$ is equal to 299; the mixture R450A is near-azeotropic, the temperature glide is equal to 0.63 K at 8.95 bar, and its $GWP_{100\text{-years}}$ is equal to 547. Both the mixtures are classified as A1 by the ANSI/ASHRAE standard. The condensation tests have been conducted in a 3.4 mm internal diameter test section that allows to visualize the flow pattern and to measure quasi-local heat transfer coefficients.

Regarding the flow pattern: at mass flux equal to 300 kg m^{-2} s^{-1} and 200 kg m^{-2} s^{-1} annular flow and stratified-wavy flow have been detected; at mass flux equal to 100 kg m^{-2} s^{-1} and 50 kg m^{-2} s^{-1}, stratified-wavy, stratified-smooth and intermittent flow have been observed.

Regarding the heat transfer coefficients, at the same mass flux and vapor quality, R515B and R450A display similar values. On average, the heat transfer coefficients of the mixture are lower compared to those of the pure fluid R1234ze(E), however, the difference is below 8%. It must be considered that this comparison is done at the same mass flux and vapor quality although pressure drop and specifically saturation temperature drop of the two fluids should be accounted for in the comparison.

The experimental database has been compared with the predictions of the Cavallini et al. (2006) and the Thome et al. (2003) models. The model by Cavallini et al. (2006) is able to predict the condensation heat transfer coefficient with a mean absolute deviation equal to 4.1 % and an average deviation equal to -3.7 %. The model by Thome et al. (2003) predicts the condensation heat transfer coefficients with a mean absolute deviation equal to 8.5 % and an average deviation equal to 5.7 %. The model by Cavallini et al. (2006) is suggested for the design of heat exchangers in which in-tube condensation takes place with mixtures R515B and R450A.

REFERENCES

Azzolin, M., Berto, A., Bortolin, S., Col, D. Del, 2022. Condensation heat transfer of R1234ze(E) and its A1 mixtures in small diameter channels. Int. J. Refrig. https://doi.org/10.1016/j.ijrefrig.2022.02.002

Azzolin, M., Bortolin, S., Del Col, D., 2019. Convective condensation at low mass flux: Effect of turbulence and tube orientation on the heat transfer. Int. J. Heat Mass Transf. 144, 118646. https://doi.org/10.1016/j.ijheatmasstransfer.2019.118646

Cavallini, A., Del Col, D., Doretti, L., Matkovic, M., Rossetto, L., Zilio, C., Censi, G., 2006. Condensation in horizontal smooth tubes: A new heat transfer model for heat exchanger design. Heat Transf. Eng. 27, 31–38. https://doi.org/10.1080/01457630600793970

Del Col, D., Bortolato, M., Azzolin, M., Bortolin, S., 2015. Condensation heat transfer and two-phase frictional pressure drop in a single minichannel with R1234ze(E) and other refrigerants. Int. J. Refrig. 50, 87–103. https://doi.org/10.1016/j.ijrefrig.2014.10.022

Diani, A., Campanale, M., Cavallini, A., Rossetto, L., 2018a. Low GWP refrigerants condensation inside a 2.4 mm ID microfin tube. Int. J. Refrig. 86, 312–321. https://doi.org/10.1016/j.ijrefrig.2017.11.011

Diani, A., Campanale, M., Rossetto, L., 2018b. Experimental study on heat transfer condensation of R1234ze(E) and R134a inside a 4.0 mm OD horizontal microfin tube. Int. J. Heat Mass Transf. 126, 1316–1325. https://doi.org/10.1016/j.ijheatmasstransfer.2018.06.047

El Hajal, J., Thome, J.R., Cavallini, A., 2003. Condensation in horizontal tubes, part 1: Two-phase flow pattern map. Int. J. Heat Mass Transf. 46, 3349–3363. https://doi.org/10.1016/S0017-9310(03)00139-X

Group 1 of the Joint Committee for Guides in Metrology (JCGM/WG1), 2008. Evaluation of measurement data — Guide to the expression of uncertainty in measurement. Int. Organ. Stand. Geneva ISBN 50, 134.

Jacob, T.A., Matty, E.P., Fronk, B.M., 2019. Experimental investigation of in-tube condensation of low GWP refrigerant R450A using a fiber optic distributed temperature sensor. Int. J. Refrig. 103, 274–286. https://doi.org/10.1016/j.ijrefrig.2019.04.021

Makhnatch, P., Mota-Babiloni, A., López-Belchí, A., Khodabandeh, R., 2019. R450A and R513A as lower GWP mixtures for high ambient temperature countries: Experimental comparison with R134a. Energy 166, 223–235. https://doi.org/10.1016/j.energy.2018.09.001

Mateu-Royo, C., Mota-Babiloni, A., Navarro-Esbrí, J., Barragán-Cervera, Á., 2021. Comparative analysis of HFO-1234ze(E) and R-515B as low GWP alternatives to HFC-134a in moderately high temperature heat pumps. Int. J. Refrig. 124, 197–206. https://doi.org/10.1016/j.ijrefrig.2020.12.023

Nusselt, W., 1916. Die Oberflächenkondensation des Wasserdampfes. VDI.

Thome, J.R., El Hajal, J., Cavallini, A., 2003. Condensation in horizontal tubes, part 2: New heat transfer model based on flow regimes. Int. J. Heat Mass Transf. 46, 3365–3387. https://doi.org/10.1016/S0017-9310(03)00140-6

AKNOWLEDGEMENTS

This work has been supported by the MiSE (Italian Ministry of Economic Development) – ENEA (Italian National Agency for New Technologies, Energy and Sustainable Economic Development) program “Ricerca di Sistema Elettrico – Piano Triennale di Realizzazione 2019–2021 – Tecnologie per la penetrazione efficiente del vettore elettrico”.
AERMEC SpA is also acknowledged for funding a researcher position